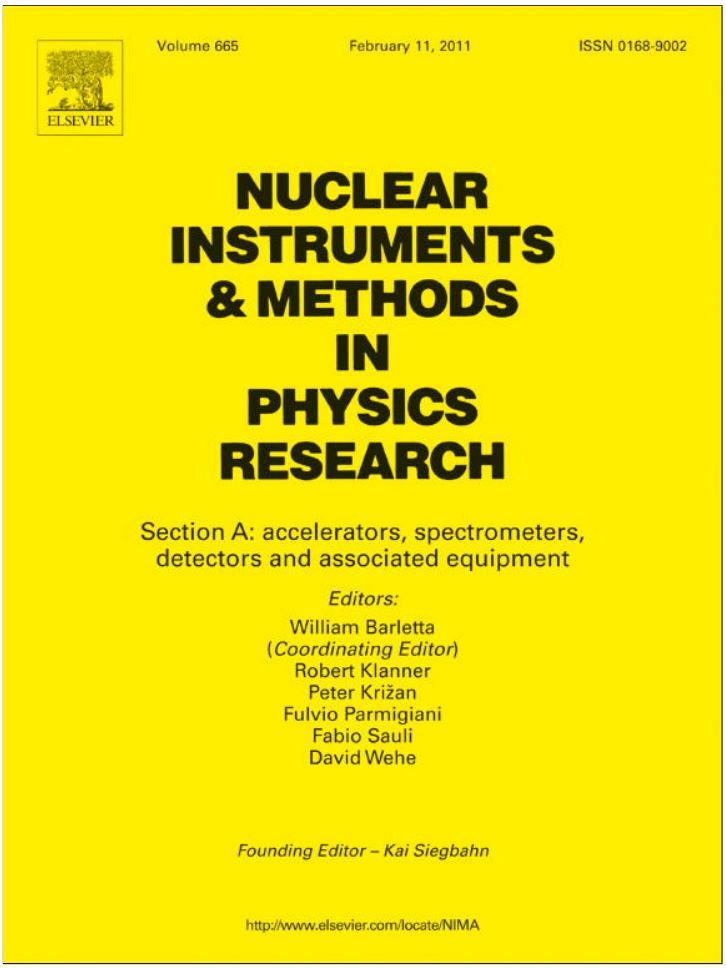

Nuclear Instruments and Methods in Physics Research A 665 (2011) 74–79

Contents lists available at SciVerse ScienceDirect

Nuclear Instruments and Methods in Physics Research A

journal homepage: www.elsevier.com/locate/nima

Detection efficiency of low levels of boron and cadmium with a $LaBr_3$:Ce scintillation detector

A.A. Naqvi [a,*], M.S. Al-Anezi [a], Zameer Kalakada [b], A.A. Isab [c], M. Raashid [a], Faris Ahmed Al Matouq [a], Khateeb-ur-Rehman [a], F.Z. Khiari [a], M.A. Garwan [a], O.S.B. Al-Amoudi [b], M. Maslehuddin [d]

[a] Department of Physics, King Fahd University of Petroleum and Minerals, Dhahran, Saudi Arabia
[b] Department of Civil Engineering, King Fahd University of Petroleum and Minerals, Dhahran, Saudi Arabia
[c] Department of Chemistry, King Fahd University of Petroleum and Minerals, Dhahran, Saudi Arabia
[d] Center for Engineering Research, King Fahd University of Petroleum and Minerals, Dhahran, Saudi Arabia

ARTICLE INFO

Article history:
Received 6 March 2011
Received in revised form
30 September 2011
Accepted 11 October 2011
Available online 12 November 2011

Keywords:
LaBr:Ce detector
Prompt gamma ray studies
Cadmium and boron concentration
Measurement in water samples

ABSTRACT

The response of a cylindrical 3 in. × 3 in. (height × diameter) $LaBr_3$:Ce detector was measured for low energy prompt gamma-rays from boron and cadmium contaminated water samples using a newly designed portable neutron generator-based Prompt Gamma Neutron Activation Analysis (PGNAA) setup. Prompt gamma-rays were measured from water samples contaminated with 0.031, 0.125, 0.250 and 0.5 wt% boron and 0.0625, 0.125, 0.250 and 0.500 wt% cadmium. The experimental yield of boron and cadmium prompt gamma-rays measured with the $LaBr_3$:Ce detector based PGNAA setup were compared with the results of Monte Carlo calculations. An excellent agreement between the experimental and calculated yields of 478 keV gamma-ray from boron and 558 keV gamma-rays from cadmium from boron and cadmium contaminated water samples, indicate an excellent response of the $LaBr_3$:Ce detector for the low energy prompt gamma-rays.

1. Introduction

Prompt Gamma-ray Neutron Activation Analysis (PGNAA) is ideally suited for in-situ elemental analysis of bulk samples in various industrial, environmental, medical and other applications [1–9]. The detection sensitivity of PGNAA setup depends upon several factors including energy resolution and efficiency of the gamma-ray detector. Conventionally high resolution HPGe detectors and NaI and BGO detectors are employed in PGNAA applications. Although HPGe detectors have higher energy resolution than NaI and BGO detectors they have lower detection efficiency as compared to NaI detector. Further HPGe detectors are very sensitive to radiation damage caused by neutrons and need extensive shielding against neutrons. Also they require cooling during operation. The HPGe detectors, which are available in smaller sizes as compared to NaI and BGO detectors, are much more expensive than NaI and BGO detectors. For these reasons, HPGe detectors are not a popular choice in PGNAA application.

Recently lanthanum-halide $LaBr_3$:Ce and $LaCl_3$:Ce series gamma ray detectors have been developed with improved energy resolution and they do not need cooling during operation. The lanthanum-halide detectors are available in large sizes and they exhibit improved energy resolution and faster light decay time compared to conventional NaI and BGO gamma-ray detectors [10–13]. For same volume, $LaBr_3$ has approximately a factor of two improved energy resolution (FWHM less than 3% at 662 keV), and 30% higher detection efficiency compared to NaI(Tl) detectors [10]. Further, the $LaBr_3$:Ce detector has faster decay time of 60 ns and can operate over wide dynamic ranges of count rate with little variation in the energy resolution [10,11]. The shortcoming of lanthanide-halide scintillators is their intrinsic activity lines, which appears as background spectral lines in their pulse height spectra. The intrinsic activity is due to the activity of the unstable La isotope contaminant present in the detectors. These intrinsic activity lines may limit the utilization of the detector, especially in low-level counting [13].

Due to their higher energy resolution and efficiency, prompt gamma-ray neutron activation analysis (PGNAA) setups employing $LaBr_3$:Ce and $LaCl_3$:Ce detectors are expected to have a better performance compared to those employing sodium iodide and bismuth germinate detectors. A cylindrical 3 in. × 3 in. (height × diameter) $LaBr_3$:Ce detector for elemental analysis of bulk samples was recently set up at King Fahd University of Petroleum and Minerals (KFUPM), Dhahran, Saudi Arabia [2,3]. The performance of the $LaBr_3$:Ce detector was tested by measuring the low energy prompt gamma-rays yield from boron- and cadmium-contaminated water samples.

* Corresponding author.
E-mail address: aanaqvi@kfupm.edu.sa (A.A. Naqvi).

0168-9002/$ - see front matter © 2011 Elsevier B.V. All rights reserved.
doi:10.1016/j.nima.2011.10.010

Boron and cadmium contamination of water samples was chosen because of their significant impact on environmental pollution. The major sources of environmental pollution of B and Cd are fertilizers, sewage sludge, manure and atmospheric deposition and manufacturing industries [14–17]. Human consumption of crops grown in soil irrigated with B and Cd-contaminated sewage over extended periods of time can cause high levels of B and Cd to accumulate in humans, which would lead to a number of illnesses [14]. Ingestion of Cd-contaminated water can induce diarrhea, severe vomiting, bone fracture (Itai-Itai disease), infertility, damage to the central nervous and immune systems, cancer development and ultimately death [16] while higher concentration of B has adverse effects on human organ, environment and the growth of agriculture product [14]. Therefore B and Cd concentration level monitoring in sewerage and irrigation water through non-destructive technique such as PGNAA is highly desired.

In this regard a portable neutron generator-based PGNAA setup was designed [18]. This setup was used to test the performance of $LaBr_3$:Ce detector in measuring the boron and cadmium concentration in the water samples. In the following text the details of the reported study is described.

2. Prompt gamma-ray yield measurement using $LaBr_3$:Ce detector

The prompt gamma-ray yields from boron- and cadmium-contaminated water samples were measured using the KFUPM portable neutron generator model MP320 PGNAA setup [14]. The PGNAA setup consists of a cylindrical specimen placed inside a cylindrical high density polyethylene moderator. The moderator has a central cylindrical cavity that can accommodate a specimen with a maximum diameter. The maximum diameter of the sample depends upon the external diameter of the polyethylene moderator. A cylindrical 3 in. by 3 in. (diameter × length) $LaBr_3$:Ce gamma-ray, with its longitudinal axis aligned along the moderator and sample's major axis, was used in this study. The $LaBr_3$:Ce gamma-ray detector model BrilLanCe 380 was supplied by Saint-Gobain crystals, Europe. The detector was coupled to a fast photomultiplier with 3 in. diameter. Also detector has a built in integrated preamplifier to process the signals. The longitudinal axis of the cylindrical sample is also at right angle with respect to the neutron beam axis. In order to prevent undesired gamma-rays and neutrons from reaching the detector, 3 mm thick lead shielding and 50 mm thick paraffin shielding were provided around the gamma-ray detector. The neutron shielding is made of a mixture of paraffin and lithium carbonate mixed in equal weight proportion. Associated with each size of the cylindrical moderator are optimum values of the specimen radius and length that can produce maximum yield of the prompt gamma-rays at the detector location. This size can be determined from the Monte Carlo calculations. The results of the Monte Carlo calculations showed that the optimum radius and length of the sample for high density polyethylene moderators with 25 cm outer diameter were 9 cm and 14.0 cm, respectively. With the PGNAA setup under consideration, the optimum values of the sample radius and length as well as outer diameter of polyethylene moderator will result in maximum yield of prompt gamma ray produced at the detector location. Fig. 1 shows the PGNAA setup with the high density polyethylene cylindrical moderator and portable neutron generator.

2.1. Measurement of LaBr:Ce detector activation spectrum

In the PGNAA studies, during the irradiation of the samples, the $LaBr_3$:Ce detector, although shielded, is also exposed to

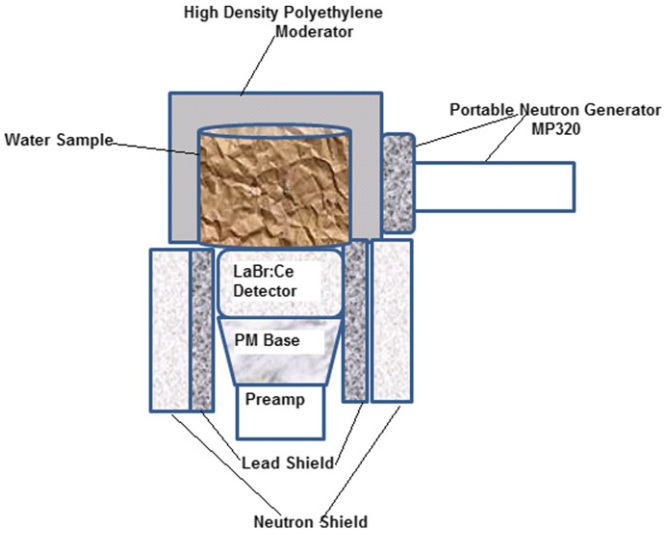

Fig. 1. Schematic representation of the MP320 portable neutron generator used to measure the prompt gamma-ray yield.

Table 1
Energies and partial elemental cross-section $\sigma_\gamma^z(E_\gamma)$-barns of prominent capture gamma-rays of boron and cadmium [19].

Element	Gamma-ray energy (keV)	$\sigma_\gamma^z(E_\gamma)$-barns
B(n,α)	478	716
Br	196	0.434
	271	0.462
	275	0.158
	315	0.460
	367	0.233
	513	0.21
	661	0.082
	828	0.285
	1248	0.0527
Cd	245	274
	558	1860
	651	359
Ce	475	0.082
	662	0.241
	1107	0.040
La	163	0.489
	272	0.502
	288	0.73
	567	0.335
	595	0.103
	789	intrinsic
	1436	intrinsic

thermal neutrons and it registers the prompt gamma-rays due to capture of thermal neutrons in La, Br and Ce elements present in $LaBr_3$:Ce detector. This activation spectrum of the detector also contains additional peaks due to intrinsic activity of the detector. Energies and intensities of prominent prompt gamma-rays due to capture of thermal neutrons in lanthanum, cerium and barium are listed in Table 1 [19]. Also, energies of gamma-rays due to intrinsic activity of the detector. All these peaks are present in the sample spectra taken with the detector and needed to be subtracted as beam associated background.

In the present study intrinsic activity and beam associated background spectra of $LaBr_3$:Ce detector were studied in detail. The detector signal was acquired using standard NIM electronics modules. The detector signal, which was routed through a preamplifier, was processed through a spectroscopy amplifier with shaping time of 1 μs. Logical gate signal was generated for each signal processed by the amplifier using single channel

analyzer and gate and delay generators modules. For dead time correction, one of the outputs of the gate and delay generator was used to gate Multichannel Buffer, while another output was used to calculate dead time correction.

Dead time DTC was calculated at the end of each experimental run from the integrated count in the stored spectrum N_{tot} and total gate signals N_{gates}. Counted independently through the relation:

$$DTC = [(N_{gates} - N_{tot})/N_{gates}]. \quad (1)$$

Then dead time corrected experimental yield of counts under a peak $Y_{DTC-Corr}$ were obtained from experimental counts under the peak Y_{exp} using the relation:

$$Y_{DTC-Corr} = Y_{exp}[1 + DTC] \quad (2)$$

Fig. 2 shows the intrinsic activity pulse height spectrum of the $LaBr_3$:Ce detector taken with a ^{137}Cs source. This figure also shows Cs peak along with intrinsic activity lines due to ^{138}La isotope. The detector has 3.3% energy resolution for 662 keV gamma-rays from ^{137}Cs. Three intrinsically produced photon peaks from the decay of La are generally observed at 32 keV, 789 keV and 1436 keV [10,11,13]. The 32 keV X-ray peak is produced by 32.2 keV K shell X-ray fluorescence of Br; where Br is produced due to the electron capture of La. The 789 keV and 1436 keV gamma lines originate from the beta decay and electron capture branches, respectively, of La [13]. In Fig. 2, only 789 keV gamma line (sitting on the beta continuum) and 1468 keV gamma-ray peak (sum line of 32 keV X-ray fluorescence peak and 1436 keV gamma line) are shown. This is in agreement with that observed in reference [13]. The abnormal width of the sum line of 32 keV X-ray fluorescence peak and 1436 keV gamma line may be due to overlapping of 1436 keV gamma line from La with 1460 keV line of ^{40}K, originating from the glass of the photo-multiplier tube [13].

The detector was exposed to fast as well as thermal neutron flux in the portable neutron generator based PGNAA setup and prompt gamma-ray yield spectrum was recorded from the detector without sample. A pulsed beam of 2.5 MeV neutrons was produced via D(d,n) reaction using 70 μA beam of 70 keV deuteron. The deuteron pulse had a width of 5 ns and a frequency of 250 Hz. Fig. 3 shows beam associated background spectrum of the $LaBr_3$:Ce detector taken during 20 min of run. Due to short irradiation time

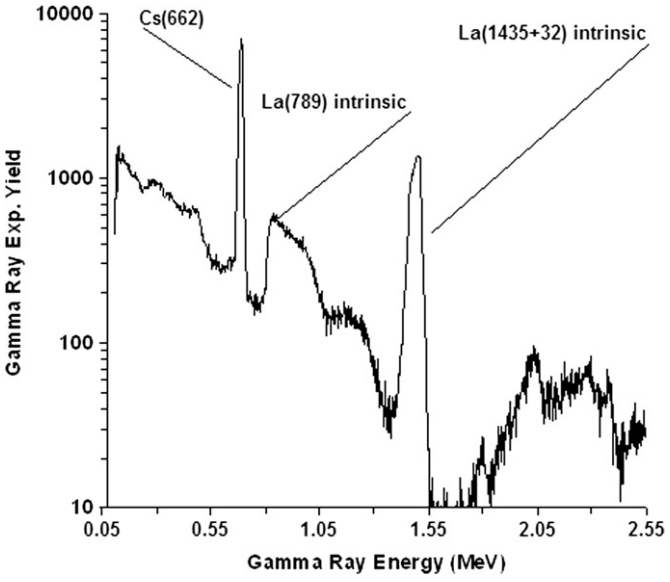

Fig. 2. LaBR:Ce pulse height spectrum taken with ^{137}Cs source exhibiting ^{137}Cs peak along with detector intrinsic activity peaks due to La.

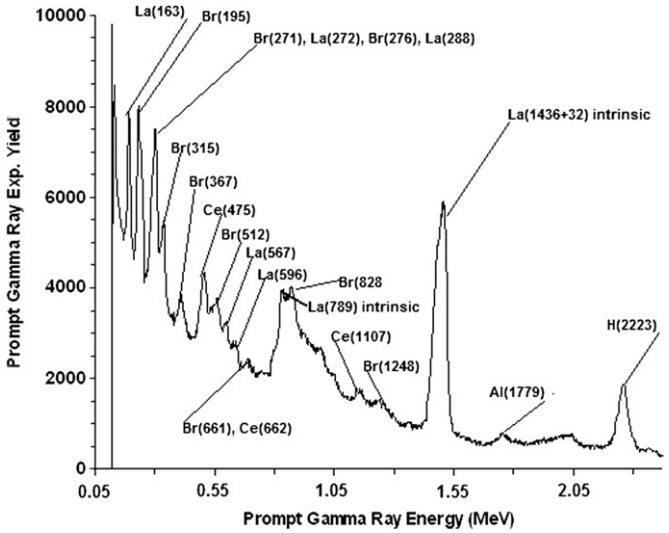

Fig. 3. Prompt gamma-ray spectrum due to activation of the LaBr:Ce detector caused by capture of thermal neutrons in La, Br and Ce elements present in LaBr:Ce detector.

delayed gamma-rays from ^{140}La (half life = 40.3 h) could not be detected. Fig. 3 shows the intrinsic activity line along with prompt gamma-ray due to activation of La, Br and Ce elements in the detector. Also shown in the spectrum is 2.22 MeV hydrogen capture peak in the moderator and neutron shielding of the detector. Most of the prompt gamma-ray lines of lanthanum, cerium and bromine listed in Table 1 have been identified in Fig. 3.

2.2. *Prompt gamma-ray analysis of boron and cadmium contaminated water samples*

The prompt gamma-ray analysis of boron and cadmium contaminated water samples was carried out using the $LaBr_3$:Ce detector. The boron and cadmium contaminated water samples were prepared by mixing boron and cadmium compounds with water. The boron and cadmium were thoroughly mixed with pure water and thereafter poured in cylindrical plastic bottles with 145 mm length and 90 mm internal diameter. Four cadmium samples with 0.0625, 0.125, 0.25 and 0.50 wt% cadmium concentration and four boron samples with 0.031, 0.125, 0.250 and 0.50 wt% boron concentration were prepared. The concentration of boron and cadmium in water samples was independently measured using Atomic Absorption Spectrometry Laboratory of Department of Chemistry, King Fahd University of Petroleum and Minerals, Dhahran, Saudi Arabia. The water samples were then irradiated in the newly designed PGNAA setup based around MP320 generator. The pulsed neutron beam was produced using the pulsed deuteron beam with specification given under Section 2.1. Pulsed neutron beam improves signal to background ratio in the PGNAA studies. The prompt gamma-ray data from boron and cadmium containing water samples were acquired for preset number of time using Multichannel Buffer based data acquisition system.

Dead time was calculated for prompt gamma-ray spectra of boron and cadmium water samples using Eqs. (1) and (2) given in Section 2.1. As expected dead time was smaller for lower concentration samples and increased with increasing concentration. For four boron samples with 0.031, 0.125, 0.250 and 0.50 wt% boron the dead time correction was calculated to be: 3.8, 5.0, 8.8 and 25%, respectively. For cadmium samples the values of dead time corrections were similar. Since the capture cross-section of cadmium is almost 2.5 times that of (n,α)

cross-section of boron, we operated neutron generator in cadmium runs with half of the beam current as compared to boron run. For four cadmium samples with 0.0625, 0.125, 0.25 and 0.50 wt% cadmium the dead time correction was measured to be: 2.5, 5.0, 8.8 and 21%, respectively.

For each boron and cadmium run the data were acquired for 25 min. Due to higher capture cross-section of cadmium, neutron generator was operated with lower flux with 35 μA beam current with 70 kV deuteron beam. Neutron flux during each run was monitored using a cylindrical 3 in. × 3 in. (height × diameter) NE213 detector with pulse shape discrimination. The NE213 detector was placed at a distance of 1.0 m from the neutron generator. The neutron detector signals were acquired through a single channel analyzer, whose lower level was set at half-Cs pulse height bias electronically set by taking Compton edge spectrum of ^{137}Cs gamma ray source with the NE213 detector. Neutron monitor spectrum was recorded for each concentration of boron and cadmium and was used for neutron flux normalization during data correction.

Fig. 4 shows pulse height spectra of prompt gamma-rays from water samples containing 0.031, 0.125, 0.250 and 0.5 wt% boron superimposed upon each other along with background spectrum taken without sample. In order to show effect of increasing concentration of boron on the pulse height spectrum, pulse height spectra for different boron concentration are plotted with a constant vertical offset. The 478 keV boron gamma-ray peak along with intrinsic 1436 keV intrinsic activity peak and 2223 keV hydrogen capture peak from moderator are quite prominent. Fig. 5 shows 478 keV boron peak on enlarged scale to show its interference with 475 keV peak from activation of cerium in $LaBr_3$:Ce detector. Since boron peaks contain the contribution of Ce(475) peak, difference spectra of boron peaks for 0.031, 0.125, 0.250 and 0.500 wt% concentration were generated by subtracting the background spectrum from each of them. Fig. 6 shows the difference spectra of boron peaks for 0.031, 0.125, 0.250 and 0.500 wt% boron concentration. Finally, the peaks of the difference spectra were integrated to generate integrated yield as a function of boron concentration.

The integrated boron yield data was corrected for dead time and neutron flux fluctuation using neutron monitor count for each boron concentration. The background of the difference spectra from the dead time corrected counts was subtracted from

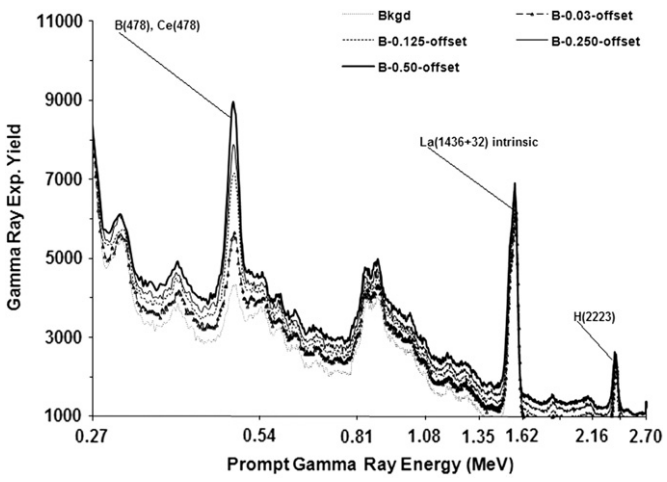

Fig. 4. Prompt gamma-rays pulse height spectra of four boron contaminated water samples containing 0.031, 0.125, 0.250 and 0.50 wt% boron. (For comparison sake background spectrum taken with pure water sample is also superimposed). In order to show effect of increasing concentration of boron on the pulse height spectrum, pulse height spectra for different boron concentration are plotted with a constant vertical offset.

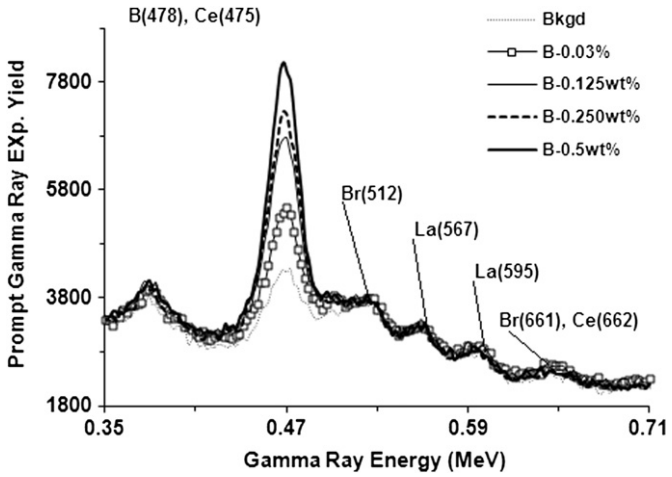

Fig. 5. Enlarged prompt gamma-ray experimental pulse height spectra of boron peak from water samples containing 0.031, 0.125, 0.250 and 0.5 wt% boron with boron showing interference of 478 keV boron peak with 475 keV Ce peak. (For comparison sake background spectrum taken with pure water sample is also superimposed).

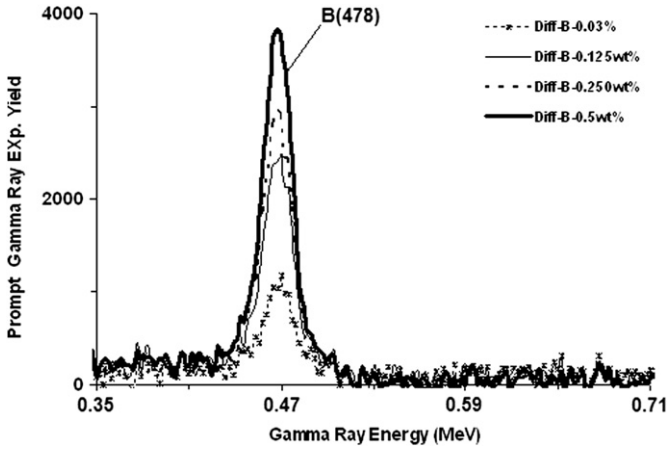

Fig. 6. Enlarged prompt gamma-ray experimental pulse height spectra after background subtraction from the four boron-contaminated water samples.

the corrected counts. The background was determined from the intercept of corrected count vs. concentration plot of the boron data. Fig. 7 shows dead time corrected and background subtracted counts of four boron samples as a function of boron concentration for boron contaminated water samples. The solid line in Fig. 7 represents results of calculated yield of prompt gamma-ray obtained from Monte Carlo calculation following the procedure described elsewhere [2]. There is an excellent agreement between the theoretical yield and experimental yield of prompt gamma-ray from boron measured by $LaBr_3$:Ce detector as a function of boron concentrations in the water samples.

Fig. 8 shows the pulse height spectra of prompt gamma rays from water samples containing 0.0625, 0.125, 0.250 and 0.500 wt% cadmium superimposed upon each other along with background spectrum taken without sample. In order to show effect of increasing concentration of cadmium on the pulse height spectrum, pulse height spectra for different cadmium concentration are plotted with a constant vertical offset. Fig. 9 shows 558 keV cadmium peak on enlarged scale to show its interference with 567 keV peak from activation of lanthanum in $LaBr_3$:Ce detector. Since the cadmium peak contains the contribution of La(567) peak, the difference spectra of cadmium peaks for 0.0625, 0.125, 0.250 and 0.500 wt% concentration were generated by

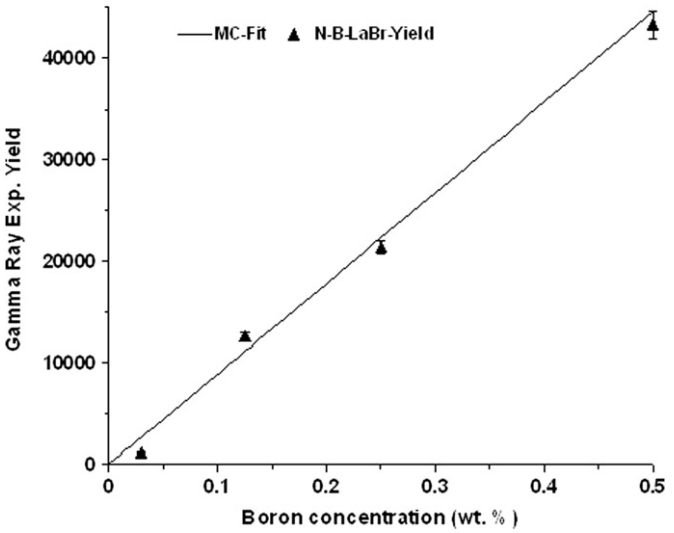

Fig. 7. Integrated dead time corrected yield of 478 keV prompt gamma-ray of boron from four water samples plotted as a function of boron concentration. The solid line shows normalized-calculated yield of the gamma-rays obtained through Monte Carlo calculations.

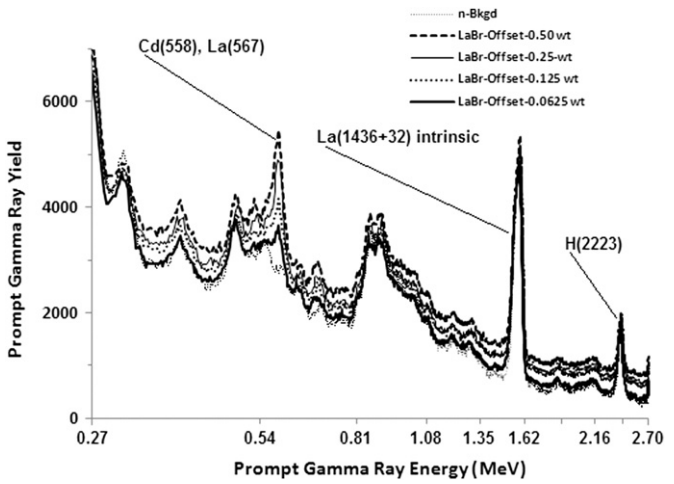

Fig. 8. Prompt gamma-ray experimental pulse height spectrum from water samples containing 0.0625, 0.125, 0.250 and 0.500 wt% cadmium showing different peaks of prompt gamma-rays produced due to the capture of thermal neutrons in the cadmium. In order to show effect of increasing concentration of cadmium on the pulse height spectrum, pulse height spectra for different cadmium concentration are plotted with a constant vertical offset.

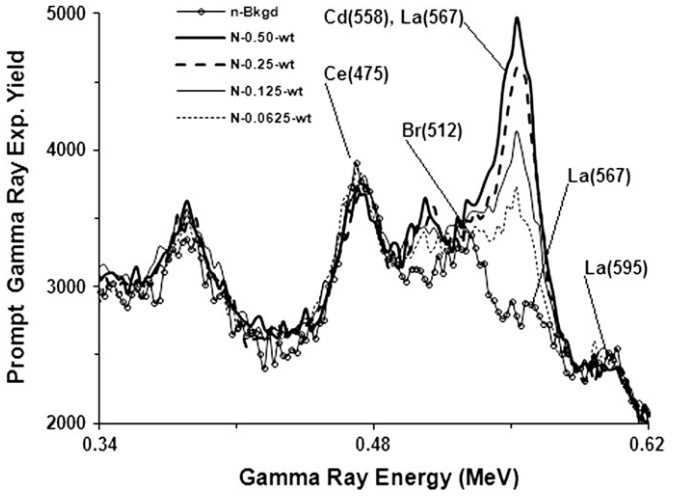

Fig. 9. Enlarged prompt gamma-ray experimental pulse height spectra of cadmium peak from water samples containing 0.0625, 0.125, 0.250 and 0.500 wt% cadmium showing interference of 558 keV cadmium peak with 567 keV La peak. (For comparison sake background spectrum taken with pure water sample is also superimposed).

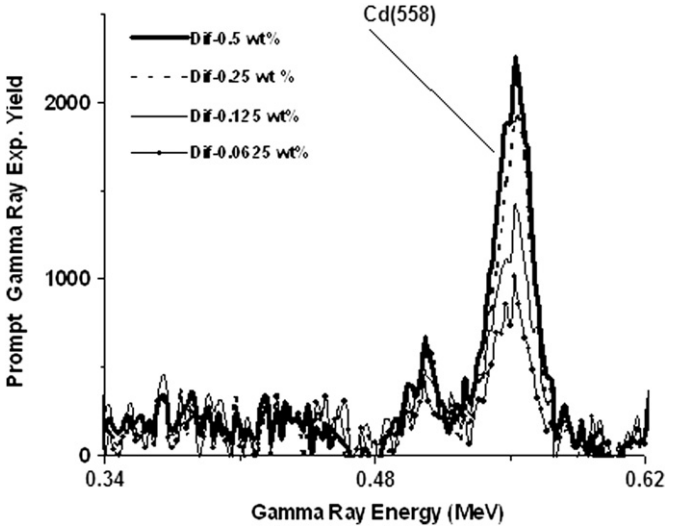

Fig. 10. Enlarged prompt gamma-ray experimental pulse height spectra after background subtraction from the four cadmium-contaminated water samples.

subtracting the background spectrum from each of them. Fig. 10 shows different spectra of cadmium peaks for 0.0625, 0.125, 0.250 and 0.500 wt% cadmium concentration. Finally, the peaks of the cadmium difference spectra were integrated, corrected for dead time correction and background of the difference spectra was subtracted following the procedure described for boron samples. Fig. 11 shows dead time corrected and background subtracted counts of four cadmium samples as a function of cadmium concentration for cadmium contaminated water samples. The solid line in Fig. 11 represents results of calculated yield of prompt gamma-ray obtained from Monte Carlo calculations following the procedure described elsewhere [2]. There is an excellent agreement between the theoretical yield and the experimental yield of prompt gamma-ray from cadmium measured by $LaBr_3$:Ce detector as a function of cadmium concentration in water samples.

2.3. Minimum detection limit of boron and cadmium in water samples

The minimum detection limit (MDC) of KFUPM portable neutron generator based PGNAA setup was determined from $LaBr_3$:Ce detector tests data following the procedure elsewhere in details [2]. For 90 mm × 140 mm (diameter × height) cylindrical water sample, minimum detection limit of boron MDC_B and its standard deviation σ_{MDCB} was calculated to be:MDC_B=30.1 ppm and σ_{MDCB}=9.3 ppm, while for cadmium minimum detection limit MDC_{Cd}=78.3 ppm and σ_{MDCCd}=23.8 ppm. Our results are in agreement with previously published results of Idiri et al. [7] for analysis of environmental cylindrical (with 40 cm diameter and 20 cm height) water samples using a 1 Ci Am-Be source based PGNAA setup utilizing 2.2×10^6 n/s. They have reported minimum detection limits for boron MDC_B=1.6 ppm and for cadmium MDC_{Cd}=6.7 ppm. We have measured higher detection limits of boron and cadmium as compared to those reported by Idiri et al. [7] because our sample volume is almost 30 time smaller than those used by Idiri et al. [7]. The volume of our PGNAA sample is

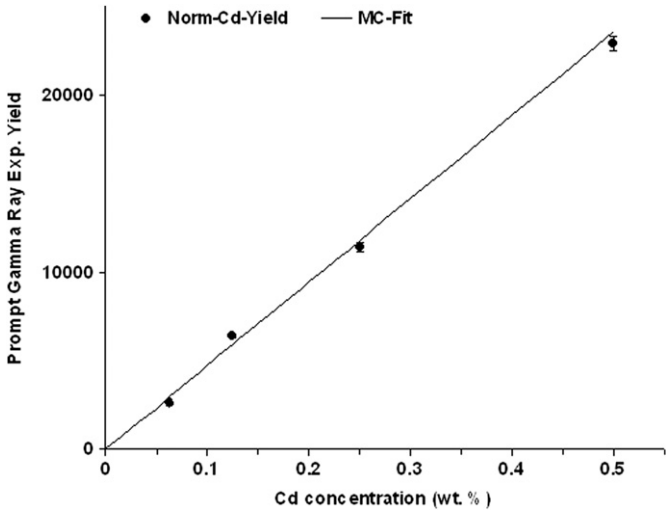

Fig. 11. Integrated dead time corrected yield of 558 keV prompt gamma-ray of cadmium from four water samples plotted as a function of cadmium concentration. The solid line shows normalized-calculated yield of the gamma-rays obtained through Monte Carlo calculations.

0.88 l while volume of PGNAA sample used by Idiri et al. [7] is 25.1 l. For the equivalent volume of the sample, we expect to achieve better MDC than reported by Idiri et al. [7].

3. Conclusions

In this study, the response of a $LaBr_3$:Ce detector was tested for the detection of low energy prompt gamma-rays from boron and cadmium contaminated water samples using a portable neutron generator spectrum. The boron concentration was varied over 0.031, 0.125, 0.250 and 0.500 wt% in water samples while cadmium concentration was varied over 0.0625, 0.125, 0.250 and 0.500 wt%. In spite of the activation during sample irradiation, the detector has excellent energy resolution to resolve boron and cadmium prompt gamma-rays from background prompt gamma-rays. The excellent agreement between the experimental yield of prompt gamma-rays with the calculated yield of prompt gamma-rays for the given concentration, shows the $LaBr_3$:Ce detector excellent performance in detecting the low energy prompt gamma-rays.

Acknowledgments

This study is part of a project no. IN090033 funded by the King Fahd University of Petroleum and Minerals, Dhahran, Saudi Arabia. The support provided by the Department of Physics, Department of Chemistry and Center for Engineering Research, King Fahd University of Petroleum and Minerals, Dhahran, Saudi Arabia is also acknowledged.

References

[1] R.L. Paul, R.M. Lindstrom, Journal of Radioanalytical and Nuclear Chemistry 243 (2000) 181.
[2] A.A. Naqvi, M. Maslehuddin, M.A. Garwan, M.M. Nagadi, O.S.B. Al-Amoudi, M. Khateeb-ur-Rehman, Nuclear Instruments and Methods in Physics Research B 269 (2011) 1.
[3] A.A. Naqvi, M. Maslehuddin, M.A. Garwan, M.M. Nagadi, O.S.B. Al-Amoudi, M. Raashid, Khateeb-ur-Rehman, Applied Radiation and Isotopes 68 (2010) 412.
[4] J.G. Fantidis, G. Nicolaou, N.F. Tsagas, A. Monte, Radiation Measurements 44 (2009) 273.
[5] J. Atanackovic, J. Grinyer, D.R. Chettle, S.H. Byun, Nuclear Instruments and Methods in Physics Research, Section B: Beam Interactions with Materials and Atoms 263 (2007) 169–174.
[6] S.L. Howell, R.A. Sigg, F.S. Moore, T.A. DeVol, Journal of Radioanalytical and Nuclear Chemistry 244 (2000) 173.
[7] Z. Idiri, H. Mazrou, A. Amokrane, S. Bedek, Section B: Beam Interactions with Materials and Atoms 268 (2010) 213.
[8] R. Khelifi, A. Amokrane, P. Bode, Section B: Beam Interactions with Materials and Atoms 262 (2007) 329.
[9] D.L. Chichester, J.D. Simpson, M. Lemchak, Journal of Radioanalytical and Nuclear Chemistry 271 (2007) 629.
[10] M. Ciema, D. Balabanski, M. Csatlo, J.M. Daugas, G. Georgiev, J. Gulya, M. Kmiecik, A. Krasznahorkay, S. Lalkovski, A. Lefebvre-Schuhl, R. Lozeva, A. Maj, A. Vitez, Nuclear Instruments and Methods in Physics Research A 608 (2009) 76.
[11] A. Favalli, H.C. Mehner, V. Ciriello, B. Pedersen, Applied Radiation and Isotopes 68 (2010) 901.
[12] A. Favalli, H.C. Mehner, F. Simonelli, Radiation Measurements 43 (2008) 506.
[13] D. Alexiev, L. Mo, D.A. Prokopovich, M.L. Smith, M. Matuchova, IEEE Transactions on Nuclear Sciences NS55 (3) (2008) 1174.
[14] K.A. Cengiz, T. Levent, Murat Dikilitas, Muhammed Ashraf, Cientia Horticulturae 121 (2009) 284.
[15] S. Baechler, P. Kudejova, J. Jolie, J.L. Schenker, N. Stritt, Nuclear Instruments and Methods in Physics Research, Section A: Accelerators, Spectrometers, Detectors and Associated Equipment 488 (2002) 410.
[16] Garcia-Reyes, et al., Microchemical Journal 82 (1) (2000) 94.
[17] B.L. Grazman, E.A. Schweikert, Journal of Radioanalytical and Nuclear Chemistry 152 (2005) 497.
[18] A.A. Naqvi, Zameer Kalakada, M.S. Al-Anezi, M. Maslehuddin, O.S.B. Al Amoudi, M. Raashid, Khateeb-ur-Rehman, M.A. Garwan, Applied Radiation and Isotopes 70 (2012) 222.
[19] Database of prompt gamma-rays from slow neutron capture for elemental analysis. Compiled by H.D. Choi, R.B. Firestone, R.M. Lindstrom, G.L. Molnar, S.F. Mughabghab, R. Paviotti-Corcuera, Zs. Revay, A. Trkov and C.M. Zhou, International Atomic Energy Agency, Vienna, 2006.